JOURNAL OF MATERIALS SCIENCE 20 (1985) 710–717

Sinterability and properties of $Ti(N_{1-x,}\ O_x)_y$–(V, Ta)C–Ni sintered alloys having a golden colour

MIKIO FUKUHARA, TETSUYA MITSUDA, YUJI KATSUMURA, AKIRA FUKAWA
Toshiba Tungaloy, Research and Development Department, 8 Shinsugita, Isogo-ku, Yokohama, 235 Japan

The effect of oxygen and carbide addition on the sinterability of TiN_y ($0.42 < y < 1$)–Ni alloys, in which part of the nitrogen is replaced by oxygen was investigated. It was found that sinterability increased as the oxygen and carbide content increased, but the strength of the resultant sintered alloys was significantly reduced due to the presence of Ni_3Ti and Ti_2O_3 phases when the oxygen content exceeded 50 mol %. The sintered alloy with the highest hardness was found when $x = 0.7$, $y = 0.78$ and the (V,Ta)C content was 18% by weight and this alloy was characterized by having a low density, good corrosion resistance and the colour of gold.

1. Introduction

Refractory hard carbides, nitrides and oxides of the transition elements in Groups IV to VI of the periodic table are characterized by having a beautiful golden colour, high corrosion resistance and hardness. When these interstitial compounds are cemented with iron group metals they are known as "cermets" and such cermets have long been used for cutting tools and decorative purposes.

TaC-based cemented alloys and TiN-coated cemented carbide which are golden in colour are now available and have been used for decorative purposes. However, TaC-based sintered alloys are unsuitable for portable decoration because of their high cost and high density ($-14.5\,Mg\,m^{-3}$). On the other hand, TiN has a low density ($5.43\,Mg\,m^{-3}$) but its sinterability is disturbed due to denitrification during the sintering process [1]. Furthermore, coated alloys are less valuable for decorative purposes due to their low toughness, colour tone variation and the tendency of coating films to peel off.

This paper will investigate the sinterability of TiN_y ($0.42 < y < 1$)–Ni mixed powder compacts using a ball milling process and subsequently the effect of oxygen and carbide addition on sinterability of TiN_y–Ni alloys with a view to producing a sintered alloy having a golden colour suitable for decorative purposes.

2. Experiment

The chemical compositions and particle size of the refractory powders used in this experiment are given in Table I.

TiN_y, $Ti(N,O)_y$ and (V,Ta)C powders were prepared from $TiN_{0.97}$ and $TiH_{1.96}$; $TiN_{0.97}$, $TiH_{1.96}$ and TiO_2, and VC and TaC, respectively. These powders were mixed in given proportions and sintered at 1673 K for 3.6 ksec in a vacuum, and subsequently reduced to powders.

These reduced powders were then ball milled with nickel powders in given proportions under acetone. The samples were heated to fixed sintering temperatures ranging from 1573 to 1723 K for 3.6 ksec under a vacuum of about 50 MPa.

Plane sections of sintered samples were prepared by diamond grinding and polishing, and the density was determined by means of Archimedes method. Hardness was measured by a Vickers tester using a 500 g load and a Rockwell tester with a 60 kg load. Transverse rupture strength at room temperature was measured with an Olsen

0022–2461/85 $03.00 + .12

TABLE I Chemical composition and grain size of powders for raw materials

Specimen	Fe	Al	Si	Cl	Mn	Mg	Ni	C	N	O	H	Particle size
$TiN_{0.97}$	–	–	–	–	–	–	–	0.21	21.22	0.28	–	1.63 μm
$TiH_{1.96}$	0.041	–	0.010	0.010	0.002	0.007	–	–	0.005	–	3.96	−350 mesh
TiO_2	0.001	0.001	–	0.005	–	–	–	–	–	–	–	−300 mesh
Ni(carbonil)	–	–	–	–	–	–	99.9	0.09	–	–	–	3.0 μm
$(V_{0.7},Ta_{0.3})C$	0.07	–	0.01	–	–	–	–	13.87	0.05	0.30	–	3.0 μm

type-universal testing machine by three point bending with a 20 mm span and a crosshead speed of 90 mm sec^{-1} using test pieces 6.5 mm × 5.2 mm × 25 mm in size. A fracture toughness (K_{Ic}) value was obtained from an indentation fracture test using a Vickers diamond pyramid indenter with a 5 kg load, and the value was calculated by using the following Equation 1 based on the median crack [2]:

$$K_{Ic} = \frac{0.203 Ha^{1/2}}{(c/a)^{3/2}} \quad (1)$$

where H is Vickers hardness, $2a$ is indentation crack length, $2c$ is the impression radius.

Young's modulus was determined by means of the pulse–echo-overlap method using an ultrasonic signal of 10 MHz. A disc specimen 24 mm in diameter and 6 mm thick was used. Dilatometric thermal expansion was determined using a sample 4 mm × 4 mm × 20 mm in size. The test was carried out in an argon atmosphere up to 1473 K at a heating speed of 300 K sec^{-1}. Thermal diffusivity was measured by a Al_2O_3–Cr^{3+} laser flash technique with a wave length of 0.6943 μm.

The disc specimens used for the measurement were 10 mm in diameter and 2 mm thick.

The colour of the sintered alloys was determined by a spectrochromometer. Phase identification was made with the aid of a microscope and an X-ray diffractometer using Cu$K\alpha$ radiation.

A corrosion resistance test was carried out at 313 K in a lactic acid solution designed to simulate sweat.

3. Results

3.1. Sintering of TiNy–Ni system

In a previous paper [3] the sintering effect of the TiN_y–Ni system was studied using nickel-plated TiN_y composite powders, however, the hardness numbers of the sintered alloys produced by this method were under 86 HRA.

In this paper the sinterability of TiN_y–Ni mixed powder compacts produced by use of a ball milling method was investigated. Contour lines of the hardness numbers obtained from these sintered alloys are given in Fig. 1 and it can be seen that the contour lines in both papers are similar except that the value of maximum hardness obtained in this paper is higher at 88 HRA.

As described in a previous paper [4] and shown in the contour lines, shrinkage during sintering is disturbed by nitrogen liberated as y, in the formula TiN_y, and the amount of nickel binder, increases. Sinterability, on the other hand, decreases as the amount of nickel binder decreases whereas TiN_y grains grow in size and hardness decreases, as y decreases.

Thus, in order to increase the hardness and to improve the sinterability, it was decided to use titanium monoxide, TiO, the colour tone and crystal structure of which, is similar to that of TiN as a sintering additive.

3.2. Sintering of $Ti(N_{1-x},O_x)_{0.85}$–Ni system

By fixing y in the formula $Ti(N, O)_y$ at 0.85, mixed powder compacts of the formula $Ti(N_{1-x},O_x)_{0.85}$–Ni were sintered at a temperature of 1773 K for 3.6 ksec in a vacuum. The theoretical density (%) and the hardness number of the sintered alloys are shown in Figs. 2a and b, respectively. The

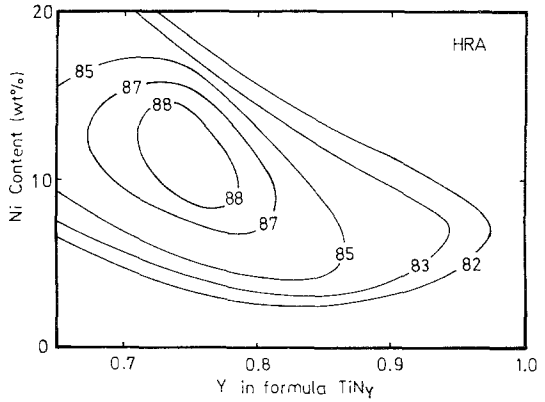

Figure 1 Hardness of sintered alloys of TiN–Ni mixed powder compacts sintered at 1733 K for 3.6 ksec in vacuum.

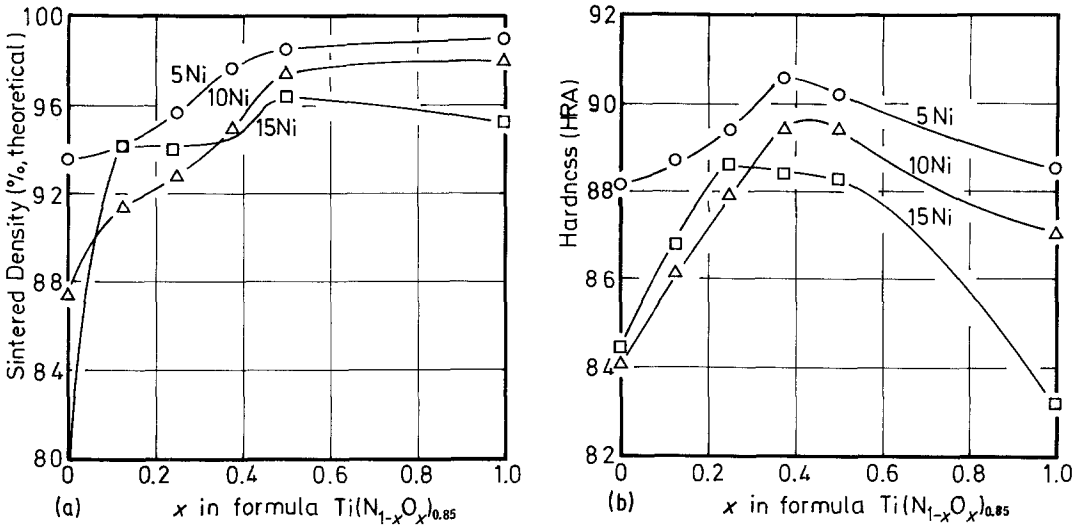

Figure 2 (a) Sintered density (%, theoretical) and (b) hardness of sintered compacts of $Ti(N_{1-x}O_x)_{0.85}$–Ni mixed powder compacts sintered at 1773 K for 3.6 ksec in vacuum.

theoretical densities of sintered alloys increase as the oxygen content increases, and, this increase can be augmented by decreasing the amount of nickel binder. The hardness of sintered alloys increases as the amount of binder decreases and shows a maximum value when the value of y is about 0.4.

Contour lines for the sintered alloys were obtained from the density curves Fig. 2a and from the hardness curves Fig. 2b, and the results tabulated in Figs. 3a and b respectively.

When the amount of oxygen exceeds 50 mol%, the strength of the sintered alloys is significantly reduced owing to exudation of nickel from the alloys, so that compositions having an oxygen content over 50 mol% were eliminated from the results shown in Fig. 3. The contour lines for both hardness and density are similar and the highest hardness and density can be found when $x = 0.4$ and the percentage of nickel in the compound is approximately 1 wt%.

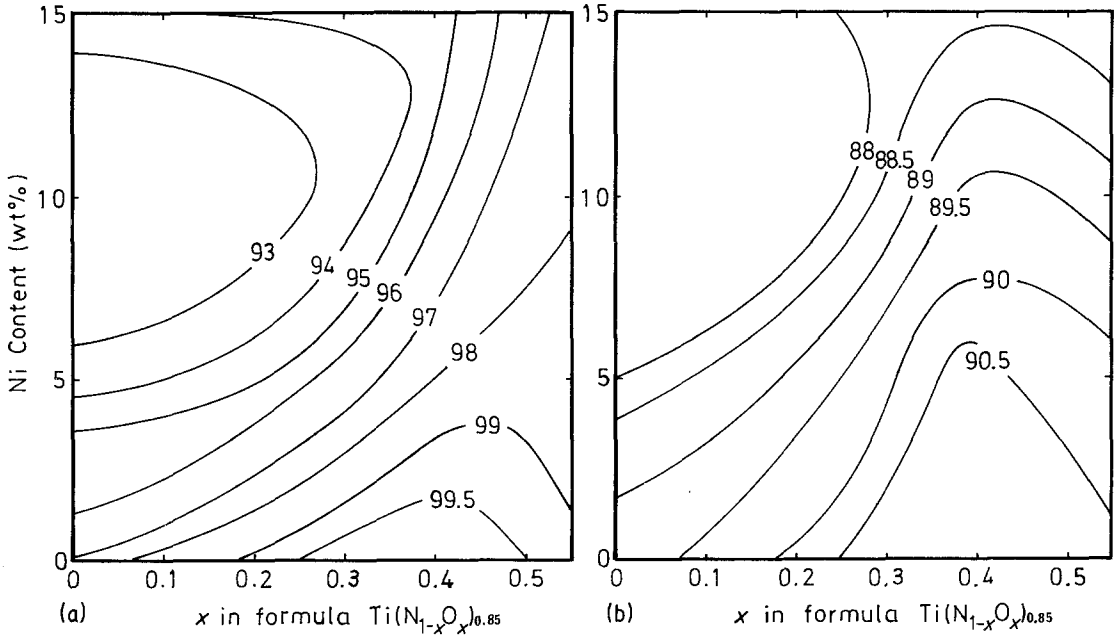

Figure 3 (a) Sintered density (%, theoretical) and (b) hardness of sintered compacts of $Ti(N_{1-x}O_x)_{0.85}$–Ni mixed powder compacts sintered at 1773 K for 3.6 ksec in vacuum.

TABLE II Chemical analysis of nitrogen, oxygen and carbon before and after sintering

Specimen	N (wt %)			O (wt %)			C (wt %)		
	Before sintering	After sintering	Variation (%)	Before sintering	After sintering	Variation (%)	Before sintering	After sintering	Variation (%)
$Ti(N_{0.6}O_{0.4})_{0.85}$	7.61	7.86	+3.3	5.46	5.90	+8.1	0.37	0.77	+108.1
$Ti(N_{0.6}O_{0.4})_{0.85}$–5 Ni	7.86	7.43	−5.5	5.61	6.24	+11.2	0.73	0.86	+17.8
$Ti(N_{0.6}O_{0.4})_{0.85}$–15 Ni	6.92	6.68	−16.6	7.10	7.06	−0.6	0.77	0.91	+18.2
$Ti(N_{0.88}O_{0.12})_{0.85}$–5 Ni	11.53	11.39	−1.2	5.33	7.61	+42.8	0.65	0.93	+43.1

A quantitative chemical analysis of nitrogen, oxygen and carbon content was carried out before and after sintering in order to explain the contour line results. These results are shown in Table II. When $x = 0.4$, $y = 0.85$ and, when the wt% of nickel is 5%, the proportion of carbon and oxygen increases and that of nitrogen decreases a little. When the wt% of nickel is increased from 5% to 15%, denitrification and deoxidation occurs.

On the other hand, when the oxygen content in the alloy is lowered, as in the formula $Ti(N_{0.88}O_{0.12})_{0.85}$, both the oxygen and carbon content increase after sintering. It is, therefore, thought that the liberation of nitrogen and oxygen, when the nickel content is high, suppresses the shrinkage of the compacts, and the sinterability decreases as the amount of nickel binder is increased, due to denitrification.

Furthermore, in the preparation of the starting material $Ti(N,O)_y$, carburization occurs during sintering, the carbide formed being titanium nitroxicarbide. However, as the amount of carbon is small it is considered as nitroxide in this paper.

From the above results it can be seen that the oxygen element promotes the sinterability of mixed powder compacts. The strength of the sintered alloy, however, deteriorates dramatically when the oxygen content is in excess of 50 mol%. It is, therefore, thought that the sintering mechanism of TiN–Ni and TiO–Ni is essentially different. Subsequently microstructures of the alloy $TiN_{0.85}$–5 wt% Ni and TiO–5 wt% Ni, which were sintered at 1773 and 1573 K respectively, for 3.6 ksec, were prepared and presented in Figs. 4a and b, respectively. The grain size of TiO in the TiO–Ni alloy is about three times larger than that of TiN_y in the $TiN_{0.85}$–Ni alloy even though the sintering temperature of the latter was 200 K lower than that of the former. Furthermore, since a number of pores can be found in the microstructure of the TiN–Ni alloy when compared with that of the TiO–Ni alloy, it is clear that the sintering effect, when oxygen is present in the alloy, is greater than when nitrogen is present in the alloy.

When the binder phase in the TiN–Ni alloy consists of a nickel solid solution alone, the X-ray diffraction pattern (shown in Fig. 5) shows that

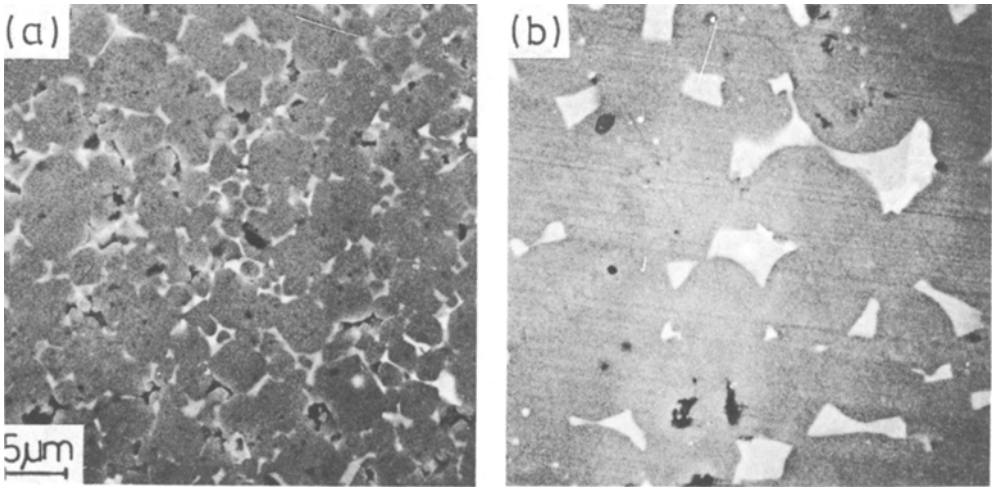

Figure 4 Microstructure of (a) $TiN_{0.85}$–5 wt% Ni and (b) TiO–5 wt% Ni mixed powder compacts sintered at (a) 1773 K and (b) 1573 K respectively, for 3.6 ksec in vacuum.

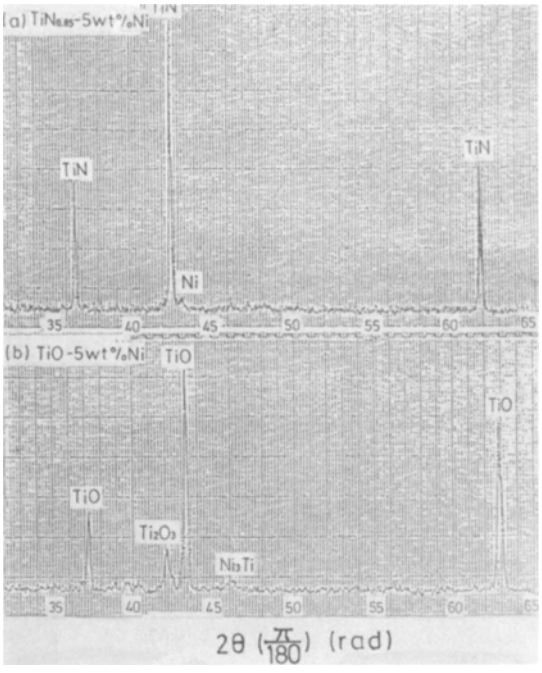

Figure 5 X-ray diffraction pattern of (a) $TiN_{0.85}$–5 wt% Ni and (b) TiO–5 wt% Ni mixed powder compacts sintered at (a) 1773 K and (b) 1573 K for 3.6 ksec.

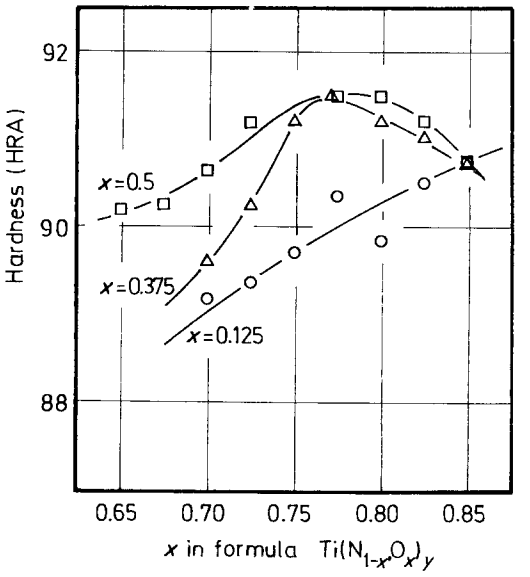

Figure 6 Hardness of $Ti(N_{1-x},O_x)_y$–20 wt% $(V_{0.7},Ta_{0.3})$C–5 wt% Ni mixed powder compacts sintered at 1773 K for 3.6 ksec in vacuum.

two new phases, Ni_3Ti and Ti_2O_3, appear instead of the solid solution in the TiO–Ni alloy. This Ti_2O_3 phase is crimson in colour and exists mostly at the boundary between the TiO grain and the binder as can be seen in Fig. 4b. The brittleness of the TiO–Ni alloy may be due to the appearance of this Ti_2O_3 phase.

3.3. Sintering of $Ti(N_{1-x},O_x)_y$–(V,Ta)C–Ni system

In the previous section, with a view to promoting the sinterability of the TiN_y–Ni mixed powder compacts, the sintering effect of oxygen, as an additive, was investigated. Notwithstanding the efficacy of oxygen, it is not possible to obtain sintered alloys having a density over 99%, and hardness in excess of 90.5 in HRA.

In order to improve the density and hardness number of the sintered alloys, y, in the formula $Ti(N_{1-x},O_x)_y$ was varied and the addition of carbides was investigated. For the choice of carbides, a double carbide of the Va group element (V,Ta)C, which is a spinodal decomposition alloy [5], was selected because it is not inclined to dissolve in the main hard phase, Ti(N,O), and to form a lower grade nitride or oxide. As can be seen from Fig. 3, since the contours of both density and hardness are similar, the hardness number serves conveniently as a measure of sinterability in place of sintered density.

The relationship between y and the hardness of sintered alloys was investigated using a mixed powder, represented by the formula $Ti(N_{1-x},O_x)_y$–20 wt% $(V_{0.7},Ta_{0.3})$C–5 wt% Ni and tabulated in Fig. 6, as an example. It can be seen that in this case the highest hardness exists when $x = 0.325$ to 0.5, $y = 0.78$.

Based on the data of Fig. 6 and other experiments it can be said that the hardness can be represented by a three-dimensional surface contour, where the oxygen content, the ratio of the non-metal element to the metal, and the amount of the carbide form the x, y and z axes, respectively. The result can be described as a half ellipsoid (see Fig. 7) in which the highest hardness (91.5 in HRA) can be found at or near the point when $x = 0.4$, $y = 0.78$ and $z = 18$.

A microstructure of a sintered alloy having a composition similar to $Ti(N_{0.6}O_{0.4})$0.775–18 wt% $(V_{0.7}Ta_{0.3})$C–5 wt% Ni is shown in Fig. 8, and it can be seen that the (V,Ta)C phase is not dissolved into the Ti(N,O) phase, and exists at or near the boundary of the Ti(N,O) grains. Therefore, the colour of the sintered alloy remains golden.

By increasing the amount of $(V_{0.7},Ta_{0.3})$C the

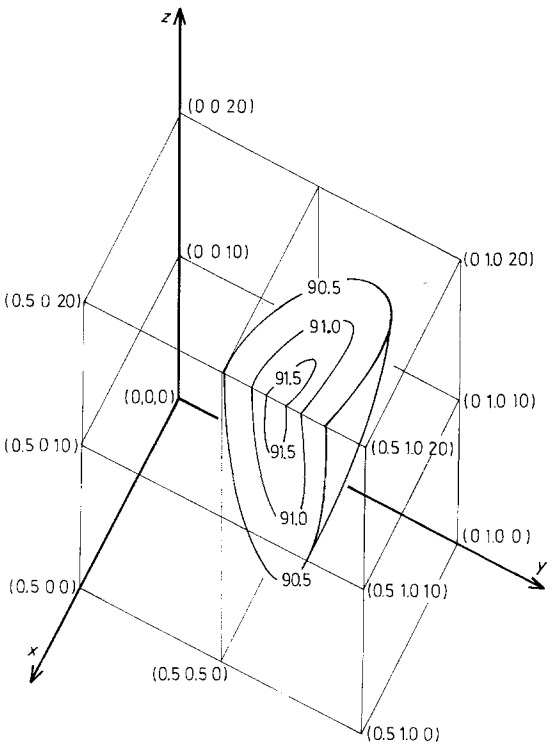

Figure 7 Hardness of sintered compacts of $Ti(N_{1-x}O_x)_y$–z wt% (V, Ta)C–5 wt% Ni mixed powder compacts at 1500° C for 3.6 ksec in vacuum.

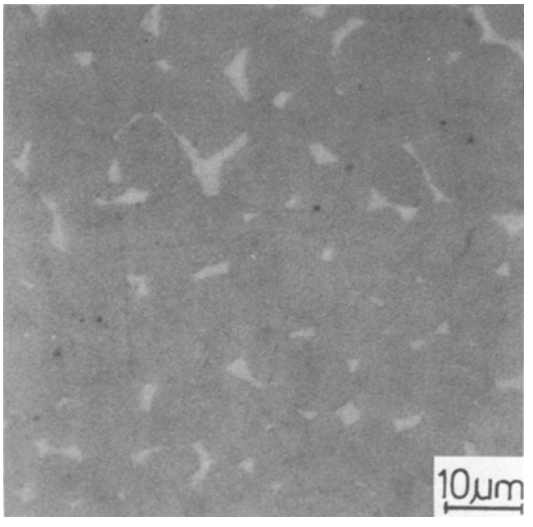

Figure 8 Microstructure of $Ti(N_{0.6},O_{0.4})_{0.775}$–18 wt% $(V_{0.7},Ta_{0.3})$–5 wt% Ni sintered at 1773 K for 3.6 ksec in vacuum.

colour varies toward a profound tone of gold, and the grain growth of the Ti(N,O) is suppressed.

3.4. Properties of the sintered alloy

Some properties of the above mentioned sintered alloy are shown in Table III. Although the transverse rupture strength and the fracture toughness of the alloy is unsatisfactory, in comparison with zirconia and silicon nitride based ceramics, it has the characteristics of low density, high hardness, good corrosion resistance and a golden colour.

4. Discussion

As shown by the contour lines of (a) density and (b) hardness in Fig. 3 the sinterability of $Ti(N,O)_y$–Ni mixed powder compacts improves remarkably as the oxygen content increases. On the other hand, the strength of the sintered alloy deteriorates significantly when the oxygen content exceeds 50 mol%.

For this reason it can be assumed that shrinkage of the compacts on heating is promoted by the ternary eutectic liquid phase involving Ti_2O_3, Ni_3Ti and a nickel solid solution as can be seen from the isothermal diagram of the Ni–Ti–O system (Fig. 9), reported by Hashimoto *et al.* [6]; and that on cooling the composition of the liquid phase changes into a three-phase field of Ti_2O_3–Ni_3Ti–TiO (see the X-ray diffraction pattern presented in Fig. 5) and subsequently Ti_2O_3 and Ni_3Ti is precipitated at the boundary of the TiO grains.

Since it is known that both phases are brittle compounds having an hexagonal structure [7], it

TABLE III Some properties of a Ti(N,O)–(V,Ta)C–Ni alloy

Density ($Mg\ m^{-3}$)	Hardness		Transverse rupture strength (MPa)	Fracture toughness K_{Ic}($MN\ m^{-3/2}$)	Corrosion resistance artificial sweat (pH 2.5 ~ 5.0)	Tone (chroma)	Young's modulus (GPa)	Thermal expansion coefficient ($10^{-6}\ K^{-1}$)	Thermal Conductivity ($J\ m^{-1}\ sec^{-1}\ day^{-1}$)
	HRA	Hv (500 g)							
5.38	91.5	1382	540.0	3.0	Not color-changed nor corroded	Golden color ($x = 0.363$, $y = 0.367$)	311.0	9.2	1.16

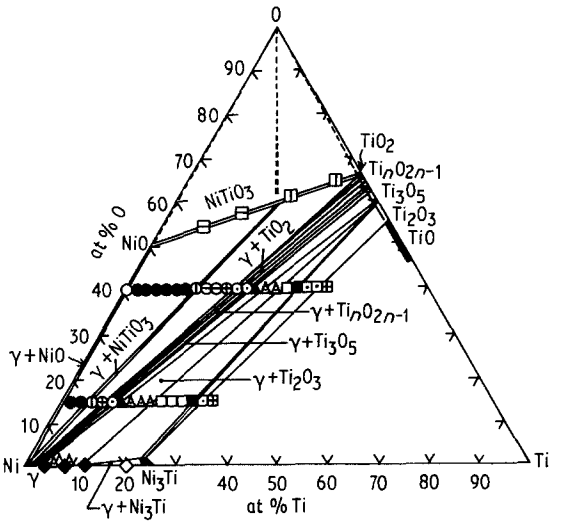

Figure 9 Isothermal diagram of the Ni–Ti–O system at 1273 K [6]: ○ $\gamma + NiO$, ⊕ $\gamma + NiTiO_3$, ⊕ $\gamma + TiO_2$, △ $\gamma + Ti_3O_5$, ▲ $\gamma + Ti_2O_3$, ■ $Ni_3Ti + Ti_2O_3$, ⊞ $Ni_3Ti + TiO$, ⊟ $NiO + NiTiO_3$, ● $\gamma + NiO + NiTiO_3$, ⊖ $\gamma + NiTiO_3 + TiO_2$, ⊙ $\gamma + Ti_nO_{2n-1}$, ▲ $\gamma + Ti_3O_5 + Ti_2O_3$, □ $\gamma + Ni_3Ti + Ti_2O_3$, ⊡ $Ni_3Ti + Ti_2O_3 + TiO$, ◇ $\gamma + Ni_3Ti$, ◆ γ, ⊡ $NiTiO_3 + TiO_2$.

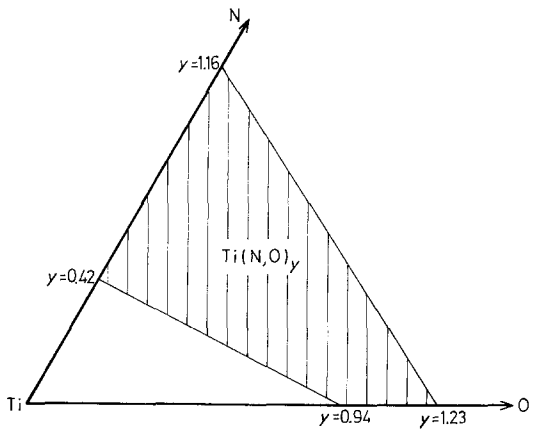

Figure 10 Isothermal diagram of the Ti–N–O system.

is considered that the occurrence of these phases is the major cause of brittleness in sintered alloys.

A titanium mononitride remains homogeneous between the values 0.42 [8] and 1.16 [9] in the formula TiN_y but a monoxide remains homogeneous over a limited range, i.e. between 0.94 and 1.23 [10] as indicated in Fig. 10. Therefore, when there are excesses of oxygen within the homogeneous range, both Ni_3Ti and Ti_2O_3 phases are formed due to the reaction of the nickel binder and a small amount of titanium in the homogeneous solid solution, hence it is necessary to prevent the oxygen content from exceeding 50 mol%.

As illustrated in Fig. 4, the grain growth of TiO in TiO–Ni is larger than that of TiN in TiN–Ni. This shows that the diffusivity of the oxygen atom in titanium is about 4 orders of magnitude as large as that of nitrogen as indicated by Sato *et al.* [11].

Although the sinterability of $Ti(N_{1-x}, O_x)_{0.85}$–Ni mixed powder compacts is improved significantly as the oxygen content increases, as shown in Fig. 2, the maximum hardness of such sintered alloys will be 90.5 HRA.

In order to improve the hardness and strength of sintered alloys, the addition of (V,Ta)C was investigated and the resultant hardness values recorded in Fig. 6. In liquid sintering of an interstitial compound, the main constituents will react with the additive compounds according to phase equilibrum, with the aid of a liquid phase. Therefore, in producing sintered alloys with a golden-colour tone it is necessary to prevent the tone from deteriorating.

In the sintering of a refractory interstitial compound of group IVa, Va and VIa elements, the stability of $[(IVa)_A, (Va)_B, (VIa)_C]\ (C_X, N_Y, O_Z)_W$ in the compound can be determined by adjusting the height of the Fermi level to the valence electron concentration (VEC) first proposed by Bilz [12].

The VEC has been defined as follows:

$$VEC = 4A + 5B + 6C + 4XW + 5YW + 6ZW$$

where A, B, C, X, Y and Z are molar fractions, W is the atomic ratio of non-metal to metal, $A + B + C = 1$ and $X + Y + Z = 1$. It can be empirically confirmed that the compound is stable when $VEC \leqslant 8.8$ and unstable when $VEC \geqslant 8.8$ under 1 atm.

In the case of an alloy having the formula $Ti(N_{0.6}, O_{0.4})_{0.78}$–18 wt% $(V_{0.7}, Ta_{0.3})C$–5 wt% Ni, the two hard compounds react with each other during sintering, and consequently a solid solution compound, having a cubic B1 structure, is formed, and the VEC parameters vary from 8.4 to 9.38 depending on the amount of renitrization and reoxidization.

As the compound is unstable when the VEC is greater than 8.8, (V,Ta)C cannot dissolve into the Ti(N,O) phase and consequently the golden colour of the sintered alloy is prevented from fading. Since the atomic ratio of non-metal to metal, W, increases as the nickel content is increased due to

the formation of a nickel solid solution, higher amounts of nickel binder will cause the VEC of the compound to exceed 8.8 so that brittle oxides of the Va group of elements precipitate from the compound, and liberated nitrogen and oxygen gases prevent the shrinkage of the specimens [1]. Therefore, the most suitable oxygen and (V,Ta)C contents exist in $Ti(N_{1-x},O_x)_y$–z wt% (V,Ta)C–Ni alloys as shown in Fig. 7. This is the main reason why the highest hardness number exists when $x = 0.4, y = 0.78$ and $z = 18$.

5. Conclusion

The effect of oxygen content and carbide addition on sinterability of $Ti(N_{1-x},O_x)_y$–Ni mixed powder compacts was investigated. The results obtained were as follows.

1. In liquid phase sintering of TiN_y–Ni alloys, the contour lines of hardness obtained from those made by means of a ball-milling process and those made by the nickel electroless plating method, are similar. However, the highest hardness that can be achieved by either method is not greater than 88 in HRA.

2. In the sintering of $Ti(N_{1-x},O_x)_{0.85}$–Ni alloys in which nitrogen in the titanium nitride is replaced by oxygen, the sinterability and grain size of Ti(N,O) increase as the oxygen content increases. However, when the oxygen content exceeds 50 mol% the strength of sintered alloys is significantly reduced owing to the occurrence of Ni_3Ti and Ti_2O_3 phases.

3. In an alloy having the composition $Ti(N_{1-x},O_x)_y$–z wt% (V,Ta)C–5 wt% Ni, the contour lines of hardness are similar to the contour surface of a half ellipsoid and the highest hardness (91.5 in HRA) can be found at or near the point where $x = 0.4, y = 0.78$ and $z = 18$. The strength of such a sintered alloy having the highest hardness is not so high, but it has the characteristics of low density, good corrosion resistance and a golden tone.

Acknowledgement

The authors wish to express their gratitude to Leslie H. Carter for helpful discussions of manuscript.

References

1. M. FUKUHARA and H. MITANI, *J. Jpn. Soc. Powder Powder Metall.* **26** (1979) 143.
2. K. NIIHARA, A. NAKAHIRA and T. HIRAI, *J. Amer. Ceram.* **67** (1984) 6.
3. M. FUKUHARA, K. TSUTSUMI and H. MITANI, *J. Jpn. Soc. Powder Powder Metall.* **27** (1980) 17.
4. H. MITANI, H. NAGAI and M. FUKUHARA, "Modern Developments in Powder Metallurgy", Vol. 14, edited by H. H. Hansner (Plenum Press, New York, 1981) p. 347.
5. R. KIEFFER, G. TRABESINGER and N. REITER, *Planseeber.* **17** (1969) 25.
6. Y. HASHIMOTO, K. KOYAMA, S. OMORI and Y. ARAMI, *J. Jpn Soc. Powder Powder Metall.* **27** (1980) 155.
7. J. R. HAGUE, J. F. LYNCH, A. RUDUICK, F. C. HOLDEN and W. H. DUCKWORTH, "Refractory Ceramics for Aerospace" (American Ceramic Society, 1964) p. 251.
8. M. P. ARBUZOV, B. V. KHAENKO and E. T. KACHKOVSKAYA, *Sov. Powder Metall.* **126** (1973) 490.
9. A. BRAGER, *Acta Physiochim. URSS* **11** (1939) 617.
10. K. IIZUMI, K. KUDAKA, T. HANAZAWA and H. KITA, *Yogyo-Kyokai-Shi* **88** (1980) 175.
11. S. SATO, K. SHINOZUKA, K. UEMATSU, N. MIZUTANI and M. KATO, *ibid.* **89** (1981) 381.
12. H. BILZ, *Z. Phys.* **153** (1958) 338.

Received 2 December 1983
and accepted 30 April 1984